

Supporting Information

Investigation on the Catalytic Behavior of one Novel Thulium-Organic Framework with Planar Tetranuclear {Tm₄} Cluster as Active Center for 5 Chemical CO₂ Fixation

Hongtai Chen,^a Zhengguo Zhang,^a Hongxiao Lv,^a Shurong Liu,^a and Xiutang Zhang^{*a}

^a *Department of Chemistry, College of Science, North University of China, Taiyuan 030051, People's Republic of China.*

E-mail: xiutangzhang@163.com

Contents

Table S1. Crystallographic data and refinement parameters of NUC-37.

Table S2. Selected bond lengths and angles of NUC-37.

Table S3. Comparison of the catalytic activity of various MOFs for the cycloaddition reaction of CO₂ with styrene oxide.

5 Figure S1. The coordination mode of tetranuclear {Tm^{III}}₄ cluster (a); the thulium-hydroxide structure (b); the coordination mode of H₅BDCP ligand.

Figure S2. TGA curve of as-synthesized (black) and activated (red) sample of NUC-37.

Figure S3. IR spectra of as-synthesized NUC-37.

Figure S4 PXRD patterns of NUC-37 before and after activation.

10 Isothermic heat calculation.

Figure S5. N₂ absorption and desorption isotherms of NUC-37a at 77 K (insert: the pore size distribution).

Figure S6. Adsorption isotherm of CO₂ at 273K and 298K.

Figure S7. CO₂ adsorption heat calculated by the virial equation of NUC-37a.

Yield calculation based on the GC-MS analysis.

15 Figure S8-S12. The ¹H NMR spectrums of cycloaddition reaction products.

Figure S13. PXRD patterns of fresh and reused NUC-37a catalyst.

Figure S14. The hot filtration experiment of cycloaddition reaction catalysed by NUC-37a.

Table S1. crystallographic data and refinement parameters of NUC-37.

Complex	NUC-37
Formula	C ₇₂ H ₆₄ N ₇ O ₃₅ Tm ₄
Mr	2263.02
Crystal system	hexagonal
Space group	P6 ₃ /mcm
a (Å)	22.120(4)
b (Å)	22.120(4)
c (Å)	38.202(8)
α (°)	90
β (°)	90
γ (°)	120
V(Å ³)	16188(7)
Z	6
Dcalcd(g·cm ⁻³)	1.393
μ(mm ⁻¹)	3.326
GOF	1.070
R ₁ [I > 2σ(I)] ^a	0.0379
wR ₂ [I > 2σ(I)] ^b	0.0969
R ₁ ^a (all data)	0.0497
wR ₂ ^b (all data)	0.1044
R _{int}	0.1094

^a $R_1 = \sum |F_o| - |F_c| / \sum |F_o|$. ^b $wR_2 = \sum w(|F_o|^2 - |F_c|^2) / \sum w(F_o)^2)^{1/2}$

Table S2. selected bond lengths and angles of NUC-37.

Tm1-O1#1	2.228(4)	Tm1-O1#2	2.228(4)	Tm1-O3	2.202(4)
Tm1-O3#3	2.202(4)	Tm1-O5#5	2.292(6)	Tm1-O5#4	2.292(6)
Tm1-O1W	2.309(4)	Tm2-O2#1	2.323(4)	Tm2-O2#7	2.323(4)
Tm2-O4	2.272(4)	Tm2-O4#8	2.273(4)	Tm2-O1W#8	2.312(2)
Tm2-O1W	2.312(2)	Tm2-O6	2.326(6)	Tm2-O2W	2.552(8)
O1#1-Tm1-O1#2	86.6(2)	O1#2-Tm1-O5#4	115.9(2)	O1#1-Tm1-O5#4	81.7(2)
O1#1-Tm1-O5#3	115.9(2)	O1#2-Tm1-O5#3	81.7(2)	O1#2-Tm1-O1W	79.72(12)
O1#1-Tm1-O1W	79.72(12)	O3-Tm1-O1#2	89.76(17)	O3#5-Tm1-O1#1	89.76(17)
O3#5-Tm1-O1#2	162.04(15)	O3-Tm1-O1#1	162.04(15)	O3-Tm1-O3#5	88.3(2)
O3-Tm1-O5#3	80.8(2)	O3#5-Tm1-O5#3	115.5(2)	O3-Tm1-O5#4	115.5(2)
O3#5-Tm1-O5#4	80.8(2)	O3-Tm1-O1W	82.32(14)	O3#5-Tm1-O1W	82.32(14)
O5#3-Tm1-O5#4	50.2(4)	O5#3-Tm1-O1W	154.89(18)	O5#4-Tm1-O1W	154.89(18)
O2#6-Tm2-O2#2	74.90(19)	O2#2-Tm2-O6	141.48(10)	O2#6-Tm2-O6	141.48(10)
O2#6-Tm2-O2W	70.5(2)	O2#2-Tm2-O2W	70.5(2)	O4-Tm2-O2#2	82.16(16)
O4#8-Tm2-O2#6	82.15(16)	O4#8-Tm2-O2#2	136.78(15)	O4-Tm2-O2#6	136.78(15)
O4#8-Tm2-O4	90.7(2)	O4#8-Tm2-O1W	147.83(16)	O4#8-Tm2-O1W#8	92.31(14)
O4-Tm2-O1W#8	147.82(16)	O4-Tm2-O1W	92.31(14)	O4-Tm2-O6	74.55(16)
O4#8-Tm2-O6	74.55(16)	O4-Tm2-O2W	67.43(19)	O4#8-Tm2-O2W	67.43(19)
O1W-Tm2-O2#2	75.30(13)	O1W#8-Tm2-O2#6	75.31(13)	O1W-Tm2-O2#6	115.80(15)
O1W#8-Tm2-O2#2	115.80(15)	O1W#8-Tm2-O1W	69.01(15)	O1W#8-Tm2-O6	75.44(16)
O1W-Tm2-O6	75.44(16)	O1W#8-Tm2-O2W	142.06(12)	O1W-Tm2-O2W	142.06(12)
O6-Tm2-O2W	124.6(3)				
Symmetry transformations used to generate equivalent atoms: #1: 2-X,1-X+Y,3/2-Z; #2: 1+Y,+X,+Z; #3: 1-Y,+X-Y,+Z; #4: 1+Y,1-X+Y,1-Z; #5: 1-Y,1-X,1-Z; #6: 2-X,1-X+Y,+Z; #7: +X,+Y,3/2-Z; #8: 1-Y,+X-Y,3/2-Z.					

Table S3. Comparison of the catalytic activity of various MOFs for the cycloaddition reaction of CO₂ with styrene oxide.

Catalyst	Catalyst (mol%)	Time (h)	Pressure (MPa)	Temp. (°C)	Yield (%)	Ref.
Rh-PMOF-1	0.2	24	0.1	100	88	S1
Zn-2PDC	0.49	3	1	80	89	S2
TCM-16 (Zr)	0.5	16	0.1	100	93	S3
[Mn ₃ L(H ₂ O) ₆ ·(DMA) ₂]	0.5	12	0.2	80	94	S4
JLU-MOF58 (Zr)	0.1	12	0.1	80	65	S5
Co ₆ (TATAB) ₄ (DABCO) ₃ (H ₂ O)	0.2	15	0.8	80	100	S6
{Ni(muco)(bpa)(2H ₂ O)}	0.5	12	0.8	80	81	S7
ZnMOF-1-NH ₂	1	8	0.8	80	88	S8
In ₂ (OH)(btc)(Hbtc) _{0.4} (L) _{0.6}	0.51	4	2	80	73	S9
NUC-37a	0.5	5	0.1	75	98	this work

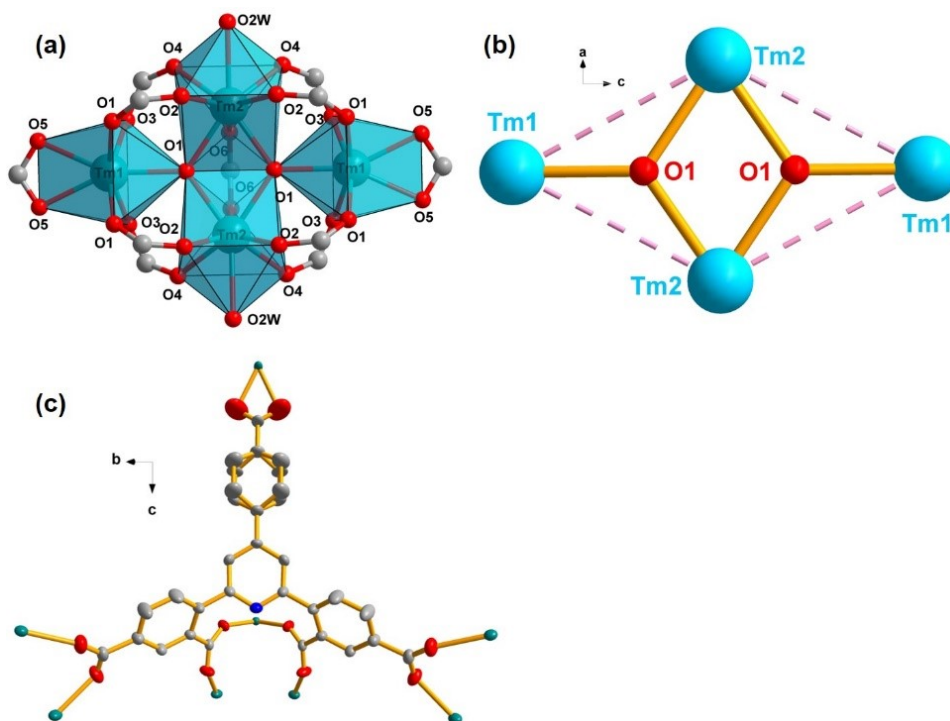


Figure S1. The coordination mode of tetranuclear $\{\text{Tm}^{\text{III}}\}_4$ cluster (a); the thulium-hydroxide structure (b); the coordination mode of H_5BDCP ligand (containing disordered C atoms) (c).

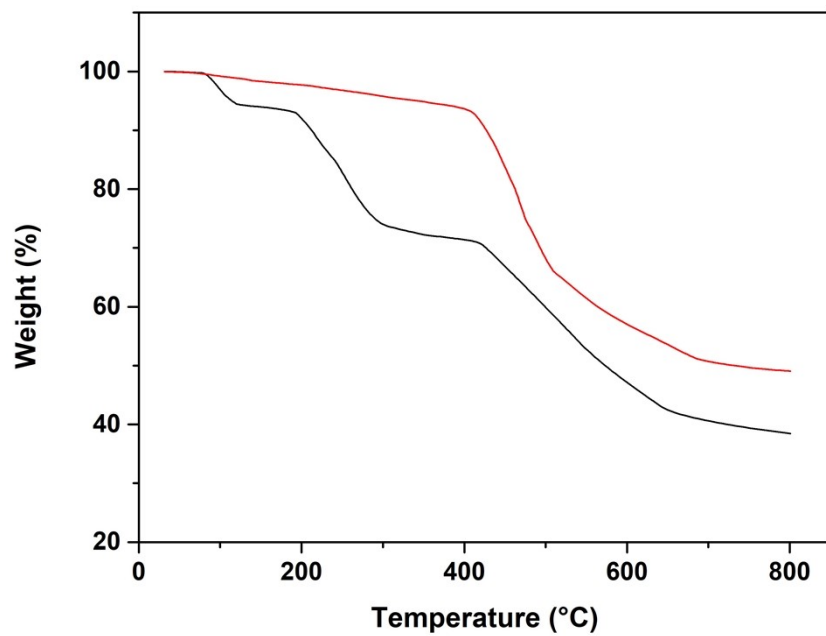


Figure S2. TGA curves of as-synthesized (black) and activated (red) sample of NUC-37.

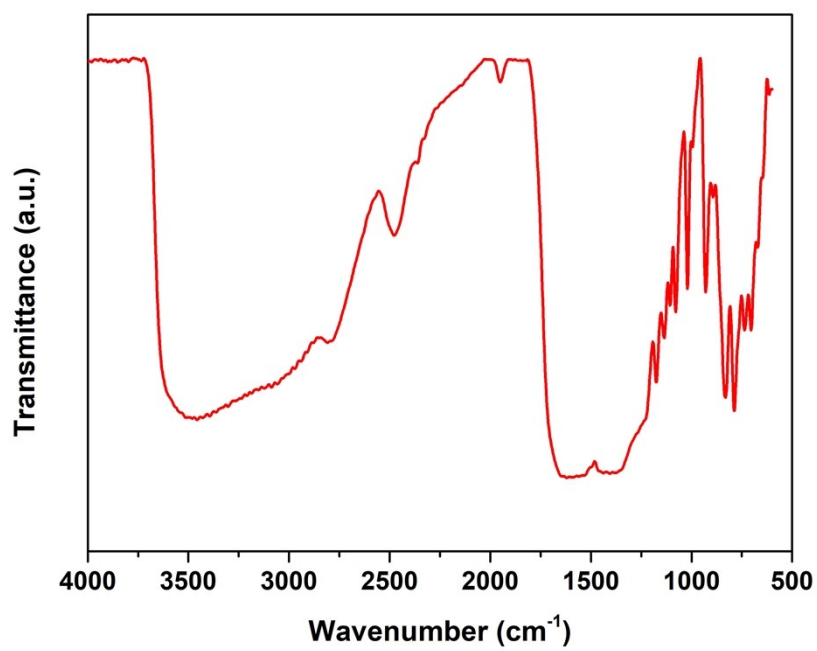


Figure S3. IR spectra of as-synthesized NUC-37.

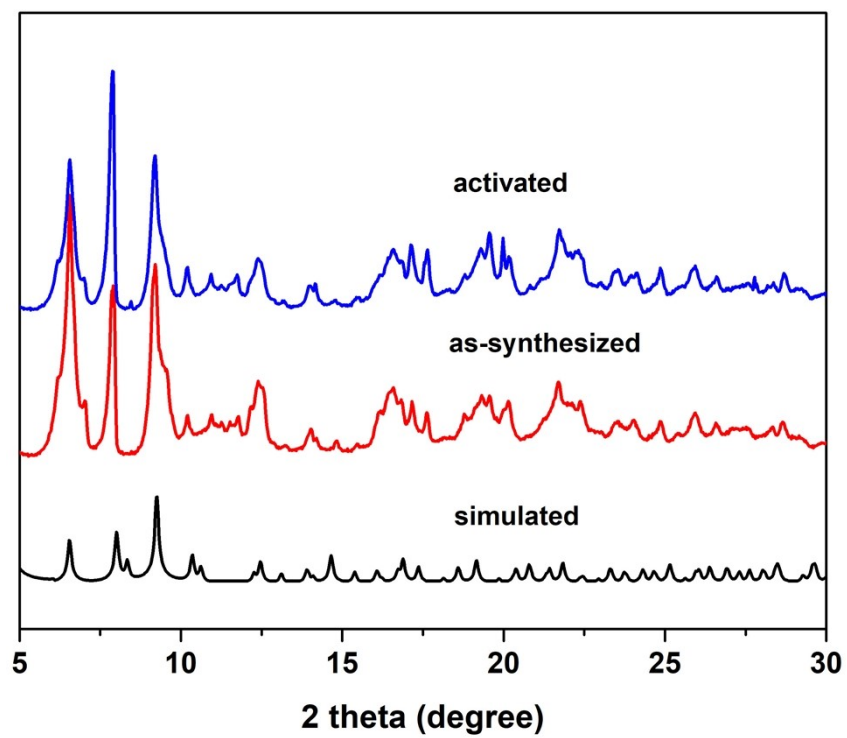


Figure S4. PXRD patterns of NUC-37 before and after activation.

Isosteric Heat Calculation.

The Q_{st} value is a parameter that describes the average enthalpy of adsorption for an adsorbing gas molecule at a specific surface coverage and is usually evaluated using two or more adsorption isotherms collected at similar temperatures. The zero-coverage isosteric heat of adsorption is evaluated by first fitting the temperature-dependent isotherm data to a virial-type expression, which can be written

5 as:

$$\ln P = \ln N + \frac{1}{T} \sum_{i=0}^m a_i N^i + \sum_{i=0}^n b_i N^i \quad (1)$$

$$Q_{st} = -R \sum_{i=0}^m a_i N^i \quad (2)$$

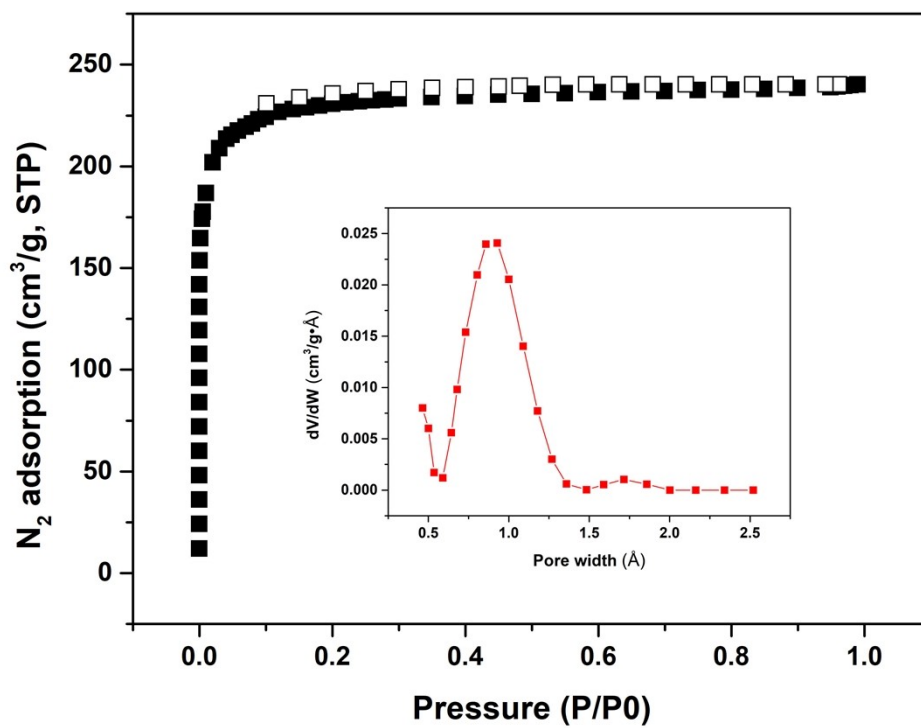


Figure S5. N₂ adsorption and desorption isotherms of NUC-37a at 77 K (insert: the pore size distribution).

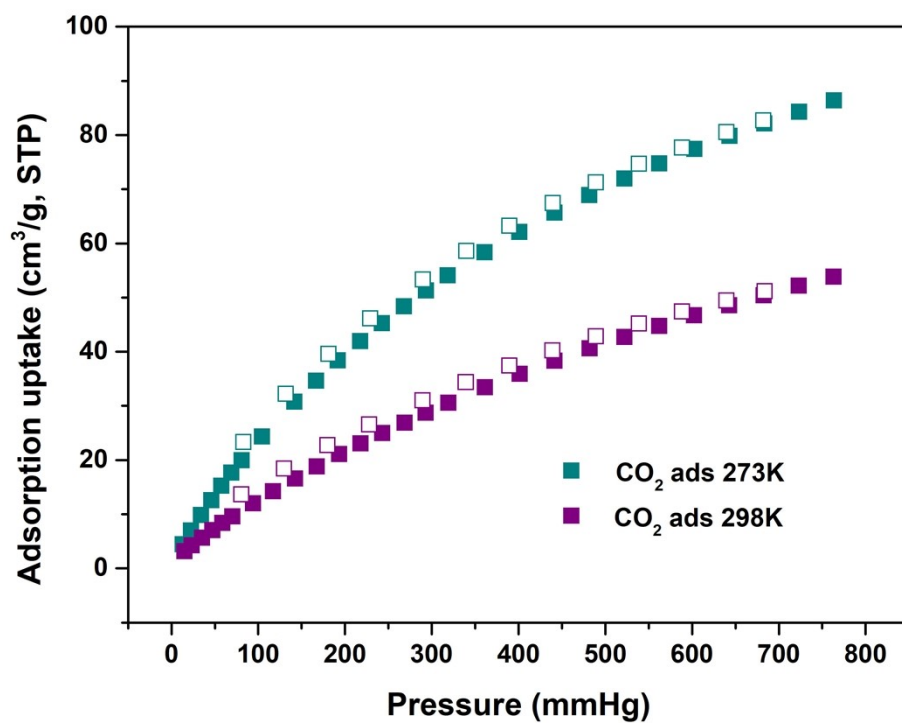


Figure S6. Adsorption isotherm of CO₂ at 273K and 298K.

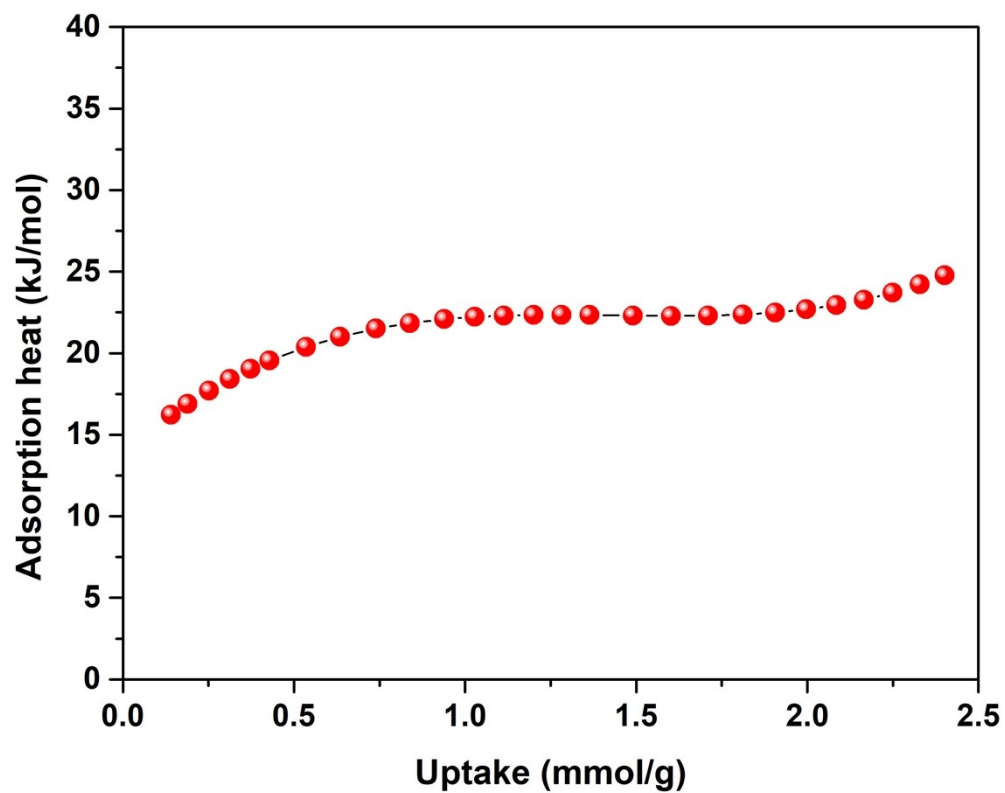


Figure S7. CO₂ adsorption heat calculated by the virial equation of NUC-37a.

Yield Calculation Based on the GC-MS Analysis

Gas chromatography mass spectrometry (GC-MS) analyses were performed on a time-of-flight Thermo Fisher Trace ISQ GC/MS instrument, the yield (%) was calculated based on the consumption of starting material using the equation:

$$5 \quad \text{Yield (\%)} = \left(\frac{\frac{\text{area of reactant at 0 hour}}{\text{area of internal standard at 0 hour}} - \frac{\text{area of reactant at any time}}{\text{area of internal standard at any time}}}{\frac{\text{area of reactant at 0 hour}}{\text{area of internal standard at 0 hour}}} \right) \times 100\% \quad (3)$$

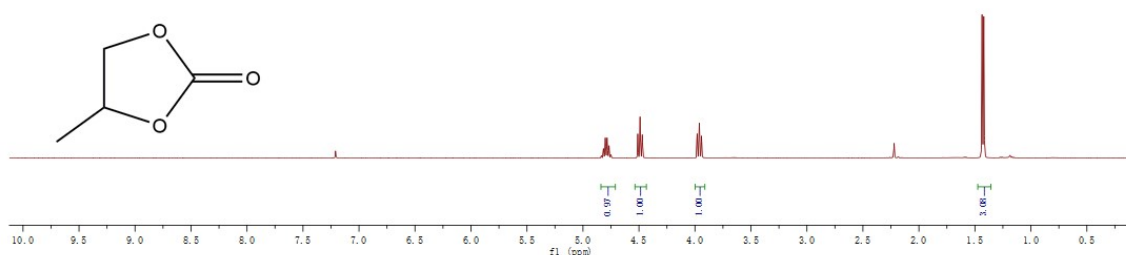


Figure S8. The ^1H NMR spectrum of 4-methyl-1,3-dioxolan-2-one (Figure 3, entry 1).

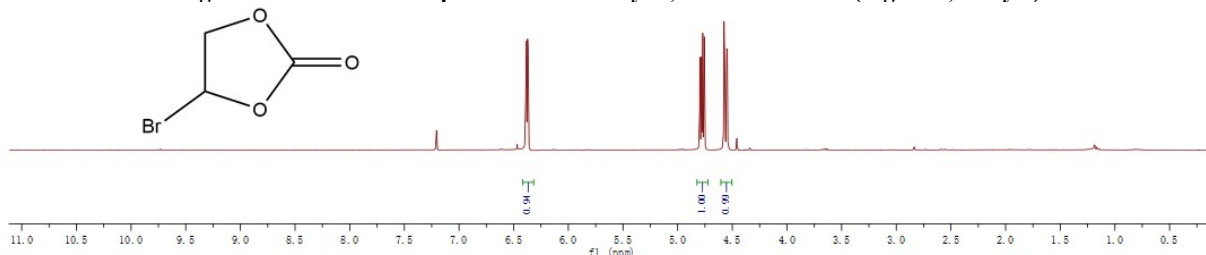


Figure S9. The ^1H NMR spectrum of 4-bromo-1,3-dioxolan-2-one (Figure 3, entry 2).

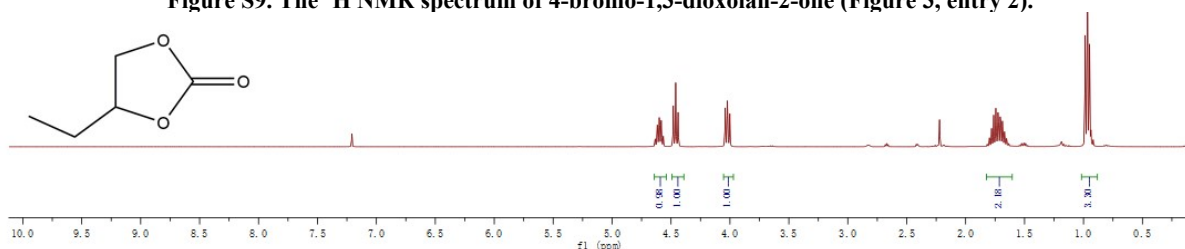


Figure S10. The ^1H NMR spectrum of 4-ethyl-1,3-dioxolan-2-one (Figure 3, entry 3).

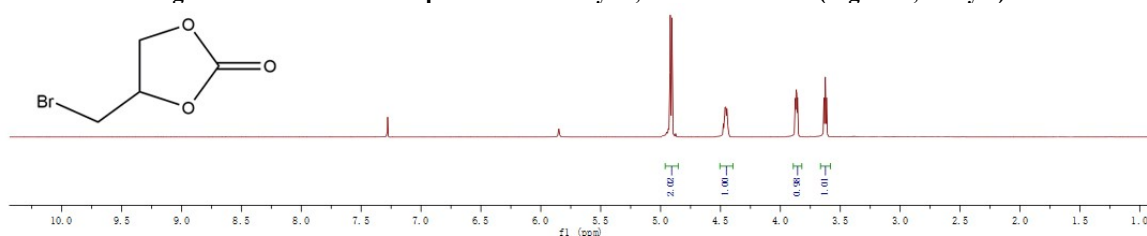


Figure S11. The ^1H NMR spectrum of 4-(bromomethyl)-1,3-dioxolan-2-one (Figure 3, entry 4).

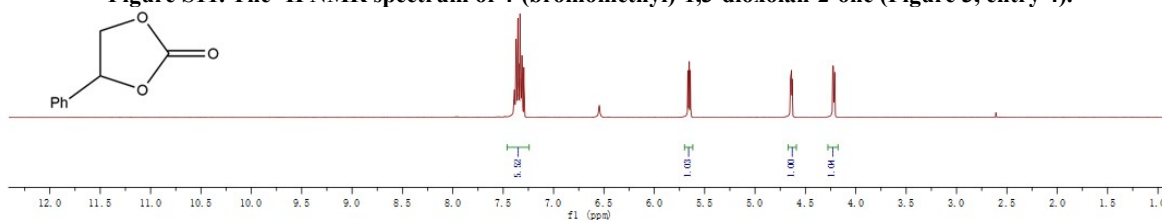


Figure S12. The ^1H NMR spectrum of 4-phenyl-1,3-dioxolan-2-one (Figure 3, entry 5).

5

10

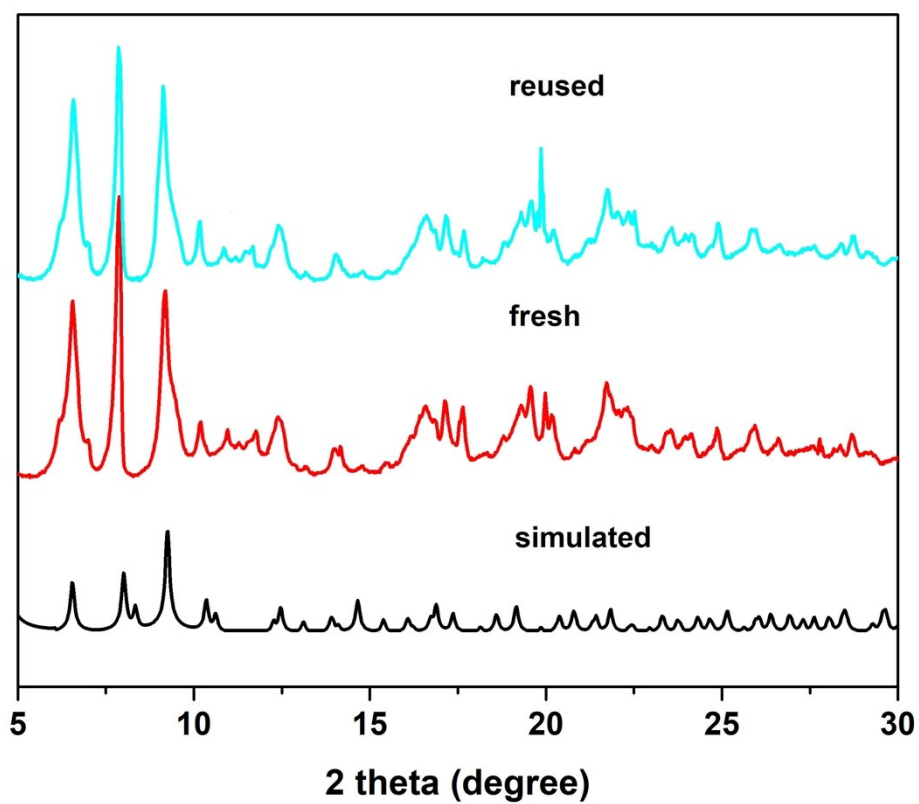


Figure S13. PXRD patterns of fresh and reused NUC-37a catalyst.

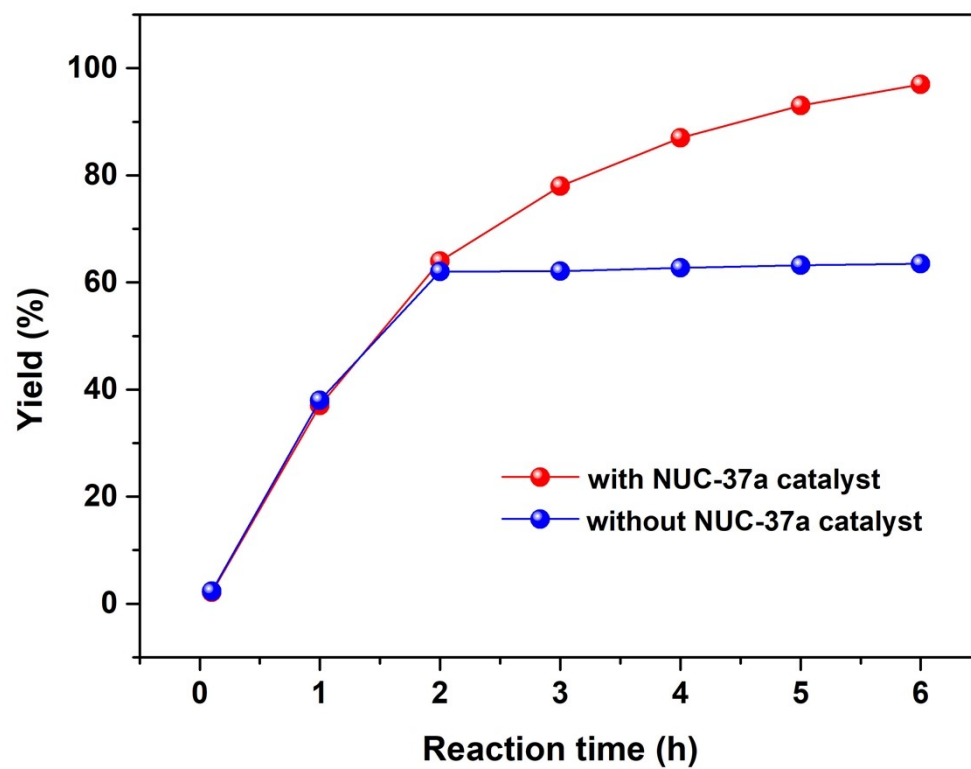


Figure S14. The hot filtration experiment of cycloaddition reaction catalysed by NUC-37a.

Reference

- (S1) J. Liu, Y. Z. Fan, X. Li, Y. W. Xu, L. Zhang and C. Y. Su, *ChemSusChem*, 2018, **11**, 2340–2347.
- (S2) Y. Li, X. Zhang, J. Lan, D. Li, Z. Wang, P. Xu and J. Sun, *ACS Sustainable Chem. Eng.*, 2021, **9**, 2795–2803.
- (S3) G. Jin, D. Sensharma, N. Zhu, S. Vaesen and W. Schmitt, *Dalton Trans.*, 2019, **48**, 15487–15492.
- 5 (S4) W. Jiang, J. Yang, Y. Y. Liu, S. Y. Song and J. F. Ma, *Chem. Eur. J.*, 2016, **22**, 16991–16997.
- (S5) X. Sun, J. Gu, Y. Yuan, C. Yu, J. Li, H. Shan, G. Li and Y. Liu, *Inorg. Chem.*, 2019, **58**, 7480–7487.
- (S6) B. Ugale, S. Kumar, T. J. Dhilip Kumar and C. M. Nagaraja, *Inorg. Chem.*, 2019, **58**, 3925–3936.
- (S7) B. Ugale, S. S. Dhankhar and C. M. Nagaraja, *Inorg. Chem.*, 2016, **55**, 9757–9766.
- (S8) P. Patel, B. Parmar, R. I. Kureshy, N. H. Khan and E. Suresh, *Dalton Trans.*, 2018, **47**, 8041–8051.
- 10 (S9) L. Liu, S. M. Wang, Z. B. Han, M. Ding, D. Q. Yuan and H. L. Jiang, *Inorg. Chem.*, 2016, **55**, 3558–3565.